ELSEVIER

Sensors and Actuators A 89 (2001) 124–134

SENSORS AND ACTUATORS A PHYSICAL

www.elsevier.nl/locate/sna

Phase-only micromirror array fabricated by standard CMOS process

Adisorn Tuantranont[*,1], Li-Anne Liew, Victor M. Bright, Wenge Zhang, Y.C. Lee

Department of Mechanical Engineering, NSF Center for Advanced Manufacturing and Packaging of Microwave, Optical, and Digital Electronics (CAMPmode), University of Colorado at Boulder, Boulder, CO 80309-0427, USA

Abstract

Smart, phase-only modulation micromirror arrays have been implemented through a commercial CMOS service. The novel, two-dimensional array of deflectable micromirrors with integrated CMOS switching circuits and piezoresistive deflection sensors on flexures is presented in this paper. The individual mirror pixel is capable of modulating light in the visible to near-infrared spectrum by piston-like movement of a trampoline-type suspended micromirror driven by thermal multi-morph actuators. A flip–chip bonding technology is used to integrate the micromirror array with a microlens array to increase the optical fill factor of the hybrid system. Analytical and finite element models verified by experiments were developed to predict and model electro-thermo-mechanical behavior of micromirror. The 2.5 mrad beam steering angle was successfully demonstrated.

Keywords: Moems; Micromirror; Bulk micromachining; Multi-morph; Phase modulation; Flip–chip

1. Introduction

The use of industrial CMOS technology enables the cointegration of mechanical microstructures with integrated circuits on the same chip. New generation of micro-electro-mechanical systems (MEMS), which is smarter and more concise is achieved by integration of digital or analog signal amplifying and processing IC circuits right next to the MEMS devices. Smart, phase-only micromirror array is a promising integrated microsystem that leads to many applications such as optical beam steering, optical data interconnect, real-time image recognition, optical interferometer, spectroscopy and aberration correction. Large deflection of micromirror is required to be able to modulate light in infrared wavelength. From many previous works on micromirrors [1–6], surface micromachining was used to fabricate parallel plate structures for electrostatically-driven segmented micromirrors and continuous-membrane deformable micromirrors. Due to a narrow gap between the electrodes in a surface micromachined process, the mirror's deflection achieved is in the range of submicrometer [1–6] or larger if the structure elevation method is used to increase the gap [7], but most is not adequate to modulate light in longer wavelength than visible spectrum. Bulk micromachined micromirror is a promising technique to solve this limitation. In this paper, a novel phase-only micromirror array including on-chip circuitry and mirror structure was fabricated through standard CMOS process using SCNA MEMS technology [8]. In addition to the long travel range, other advantages of our CMOS micromirror include low cost, high yield, mass production, and easy integration of digital or analog electronics in a standard integrated circuit process.

The thermal multi-morph actuator, which is a multi-layer structure of metal and polysilicon encapsulated with silicon dioxide is easily fabricated using all the materials available in the standard CMOS process and is used to actuate micromirror. Due to the differences of thermal expansion coefficient (CTE) of the stacked materials comprising the actuator, the beam curls and deflects the attached mirror when a resistive heating from input electrical power is applied.

As a thermally-activated mechanical device, the fundamental issues of interest are the steady-state temperature increase and distribution as a result of the electro-thermal heating, and the resulting deflection of the mirror.

Many analytical models exist that describe the behavior of bimorph and multi-morph beams [9–11]; however, the actuator used in our device is not a pure bimorph or multi-morph cantilever beam because its cross section is not uniform along its length, nor are all the important layers in the flexure of the same length. Therefore, an

[*] Corresponding author. Tel.: +1-303-735-1763; fax: +1-303-492-3498.
E-mail address: adisorn.tuantranont@colorado.edu (A. Tuantranont).
[1] URL: http://mems.colorado.edu.

0924-4247/01/$ – see front matter
PII: S0924-4247(00)00544-6

electro-thermo-mechanical model need to be developed to characterize the specific actuator structure of the described micromirror.

Two steps were taken to model the static deflection of the thermally-actuated micromirror. The first step consisted of extending the existing bimorph-beam theory to take into account the unique geometrical features of the flexures. The second step used finite element analysis to determine the effects of the temperature distribution on mirror deflection. Then, the model was verified by experimental results.

The usefulness of the micromirror device for optical beam steering applications is demonstrated through the 2.5 mrad beam steering angle.

2. CMOS micromirror

The novel two-dimensional array of deflectable micromirrors (Fig. 1) is fabricated by the orbit 2 μm double polysilicon, double metal CMOS process, available through the MOS implementation service (MOSIS) [8]. The micromirror is designed to modulate light in the visible to near-infrared wavelengths by piston-type movement of micromirror. The individual mirror pixel consists of a $40\,\mu m \times 40\,\mu m$ trampoline-type micromirror plate suspended by thermal multi-morph flexures at each corner, as shown in Fig. 2(a). The suspended micromirror plate composes of stacked aluminum commonly available in standard IC processes. The aluminum shows a high optical reflectivity (>90%) over operation wavelengths. The micromirror plate and multi-morph actuators are coupled with an oxide spring beam. The thermal multi-morph structures consist of polysilicon resistor wires and aluminum layers encapsulated in SiO_2, as shown in Fig. 2(c). Due to the different coefficients of thermal expansion of multi-layer sandwich of different materials, the flexures curl when an ohmic heating from the input electrical power is applied [11], thus causing piston-type motion of the micromirror plate. The array is anisotropically etched in EDP solution to release the micromirror structure. A pit is formed under the suspended pixel structure, giving high degree of thermal isolation from the surrounding substrate. Piezoresistive deflection sensors, as shown in Fig. 2(b), are integrated on flexures of each micromirror to provide feedback control of the position of each micromirror to improve device performance in real-time. Integrated CMOS switching circuit adjacent to each pixel, as shown in Fig. 3, works as switching ''and'' gate allowing the current go into the row and column addressed pixel. The switching circuit allows to address the pixel by 5 V data pulses and operate in digital mode. The multi-morph beam is 72 μm long, 14 μm wide and 4.175 μm thick with 2.8 μm wide and 0.4 μm thick polysilicon heater wire running between aluminum layer and oxide layer to generate heat. The ends of multi-morph actuator beams are coupled to the micromirror plate with the oxide beams (21 μm long, 7 μm wide and 3 μm thick). After the anisotropic silicon etching has undercut and released the cantilever beams, the beams curled up out of the substrate plane due to internal stresses in their thin structural layers. The etched micromirror plate is thus elevated above the substrate plane by 0.5 μm. The flatness of the micromirror is measured using white light interferometric microscope. The peak-to-valley of the unactuated micromirror is 0.22 μm ($\approx\lambda/20$ of maximum operating wavelength). And the flatness of the actuated micromirror is not significantly changed by measurement.

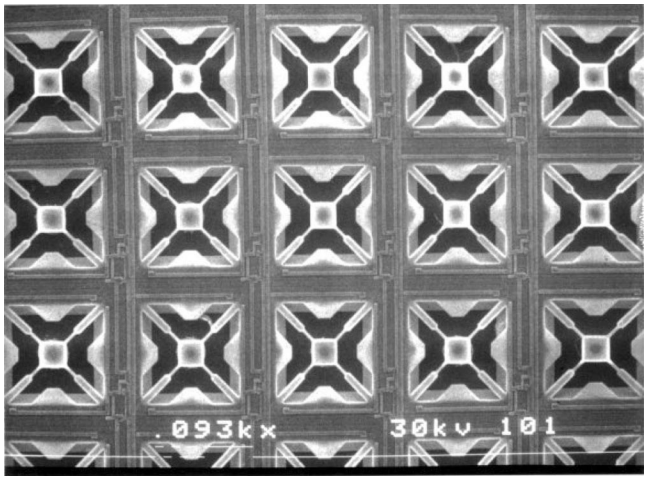

Fig. 1. A portion of smart phase-only modulation micromirror array.

3. Design analysis

3.1. Analytical modeling

In previous works [11,12], MEMS thermal actuators have been modeled using bimorph theory. In our device, multi-morph beams, which consist of layers (more than two layers) of material sandwiched together to form a composite beam were used. And the fact that the actuator's end was not free but is constrained by the mirror plate is considered. Two assumptions for which bimorph and multi-morph beam theory was previously developed are (I) each layer comprising the structure is the same length, which is the total beam length, and (II) the cross section is constant for the entire length of beam. Our CMOS micromirror flexure violates these two major assumptions. Not only is the cross section nonuniform, but the heating polysilicon resistor and the aluminum layer also do not span the entire length of the beam, meaning that the actuation effect takes place only along part of the flexure. These deviations from classical bimorph beam effect the power consumption, and thermal response time, and also complicate the use of bimorph theory because of the additional mechanical coupling and change in moment of inertia.

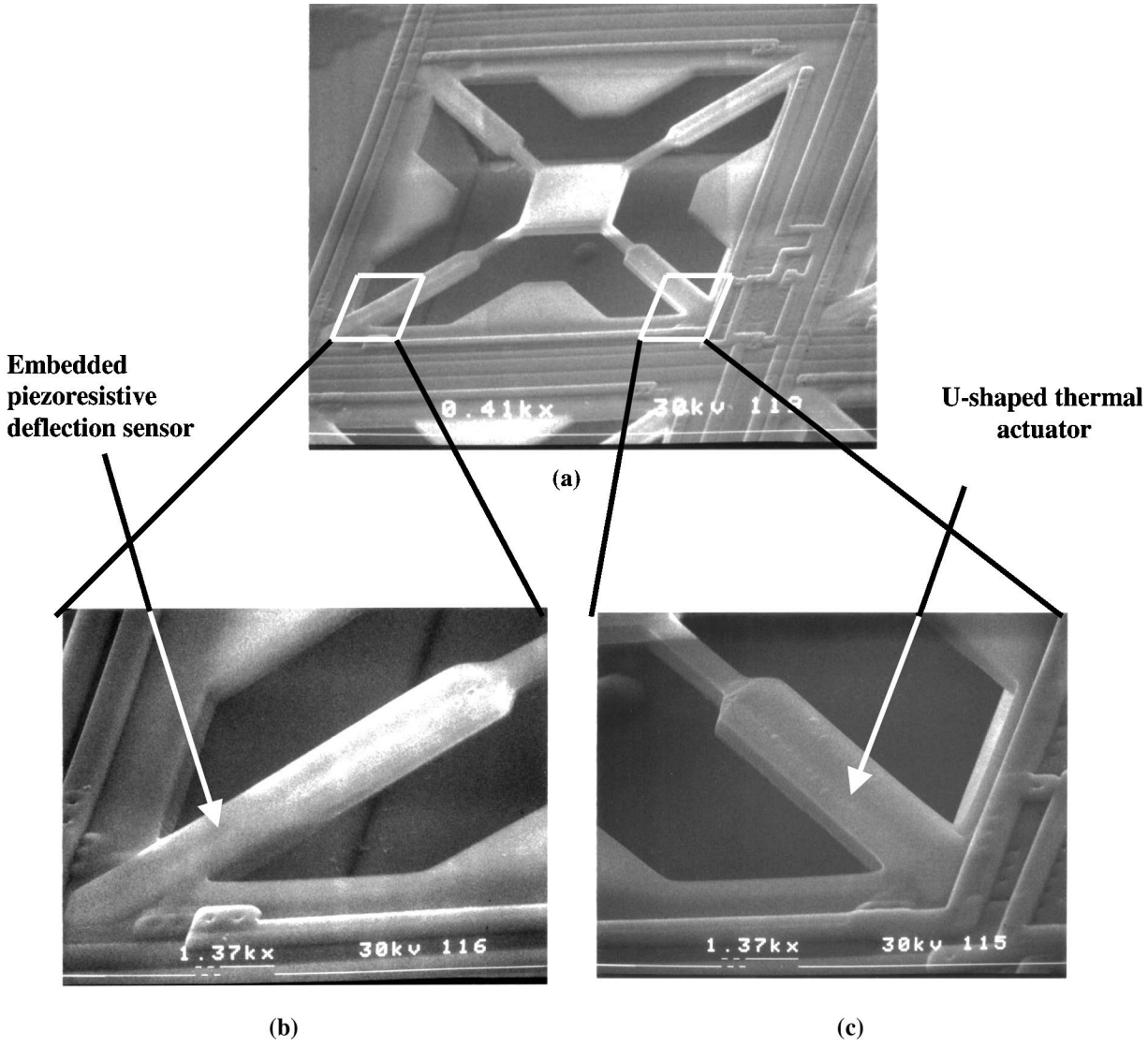

Fig. 2. Scanning electron micrograph of a pixel of micromirror (a); close-ups of flexures, including embedded resistor for piezoresistive deflection sensor (b) and embedded polysilicon wire in thermal multi-morph actuator (c).

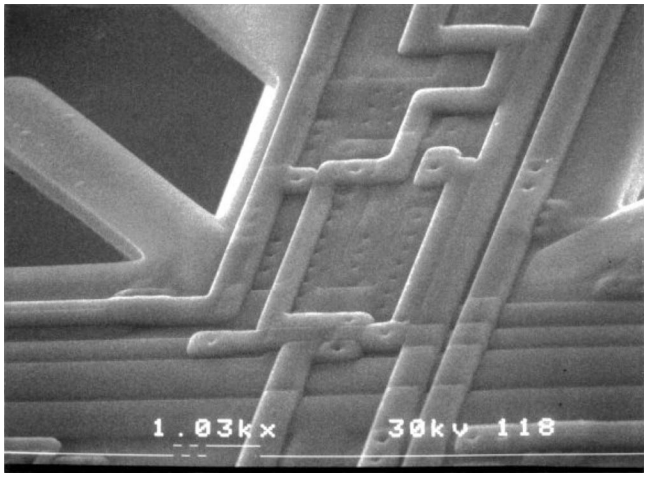

Fig. 3. Integrated CMOS switching circuit adjacent to each pixel for digital mode operation of the micromirror.

For the propose of modeling, the flexure was divided into two separate beam segments, one containing the heating elements, which is a classical bimorph cantilever, and the additional segment that connects the bimorph to the mirror plate as shown in Fig. 4. The temperature increase from the accompanying finite element model was used together with bimorph beam equations to calculate the effective force at the tip of the bimorph cantilever as it curls downward due to the thermal expansion mismatch. A nodal displacement method [13] was then used to obtain the deflection of the attached segment.

Since the thickness of the heating resistor is small compared to the thickness of the encapsulating oxide, the thermal actuation of the micromirror flexure can be modeled as a bimorph [11], where t_1 is the thickness of the silicon dioxide and t_2 is the thickness of the aluminum. From bimorph beam theory [9–10], the curvature due to the

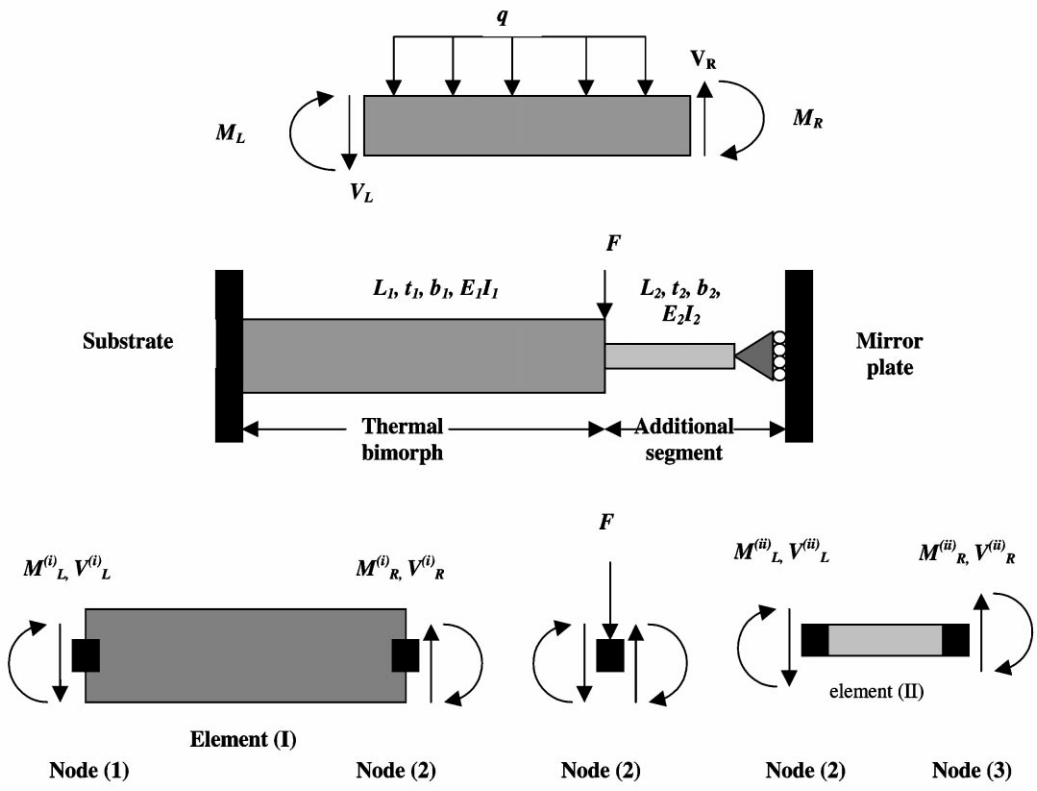

Fig. 4. Schematic of nodal displacement method applied to micromirror flexure. The flexure is considered as two beam elements connected at node 2. Shear force and bending moments acting on each node are indicated.

thermal expansion mismatch is

$$\kappa = \frac{6b_1b_2E_1E_2t_1t_2(t_1+t_2)(\alpha_1+\alpha_2)\,\Delta T}{(b_1E_1t_1^2)^2+(b_2E_2t_2^2)^2+2b_1b_2E_1E_2t_1t_2(2t_1^2+3t_1t_2+2t_2^2)} \tag{1}$$

where E is Young's modulus, α the coefficient of thermal expansion, b the width, and t the thickness of each layer, denoted by the subscript, and ΔT the change in temperature from the ambient. The deflection of the free end of the bimorph is

$$d = \frac{\kappa L^2}{2} \tag{2}$$

where L is the length of the bimorph. Using the transformed section method, the flexural rigidity of the composite beam is [14]

$$EI_{\text{bimorph}} = \frac{(t_1^2b_1E_1)^2+(t_2^2b_2E_2)^2+2t_1t_2b_1b_2E_1E_2(2t_1^2+2t_2^2+3t_1t_2)}{12(t_1b_1E_1+t_2b_2E_2)} \tag{3}$$

Then, the force generated by the tip of the bimorph as it curls downward is

$$F = \frac{3EI_{\text{bimorph}}d}{L^3} \tag{4}$$

Using a nodal displacement method for beam bending, the entire flexure is then considered as two elements connected at a common node, as indicated in Fig. 4.

For a single beam element undergoing pure bending, the shear force V and moment M at each node can be determined in terms of the nodal displacements y and slopes y' as [14]

$$\begin{aligned}
V_{\text{L}} &= \frac{EI}{L^3}(-12y_{\text{L}}-6Ly'_{\text{L}}+12y_{\text{R}}-6Ly'_{\text{R}})+\frac{qL}{2},\\
V_{\text{R}} &= \frac{EI}{L^3}(-12y_{\text{L}}-6Ly'_{\text{L}}+12y_{\text{R}}-6Ly'_{\text{R}})+\frac{qL}{2},\\
M_{\text{L}} &= \frac{EI}{L^2}(-6y_{\text{L}}-4Ly'_{\text{L}}+6y_{\text{R}}-2Ly'_{\text{R}})+\frac{qL^2}{12},\\
M_{\text{R}} &= \frac{EI}{L^2}(-6y_{\text{L}}+2Ly'_{\text{L}}-6y_{\text{R}}+4Ly'_{\text{R}})+\frac{qL^2}{12}
\end{aligned} \tag{5}$$

where q is a distributed load applied along the length of the beam, which in this case is 0. In our case, equilibrium conditions at node 2 give the following two equations:

$$-V_{\text{R}}^{(i)}+V_{\text{R}}^{(ii)}-F=0, \qquad M_{\text{R}}^{(i)}=M_{\text{L}}^{(ii)} \tag{6}$$

where the superscript refers to the elements, and the subscript refers to the nodes. At node 3,

$$V_{\text{R}}^{(ii)}=0, \qquad M_{\text{R}}^{(ii)}=0 \tag{7}$$

The equilibrium equations can be re-written using the expressions in Eq. (5). The following boundary conditions

were applied: at node 1, $y = 0$ and $y' = 0$, because this is the fixed end of the cantilever; at node 3, $y' = 0$ and the moment is 0, because it was assumed that the plate does not bend or exert a bending moment on the flexure. Then, the displacement of node 3 can be solved as

$$y_3 = -\frac{1}{6}L_2F \times \left[\frac{3k_b^{(i)} + k_b^{(ii)}}{3k_b^{(i)}k_a^{(i)}L_1 + k_b^{(i)}k_a^{(ii)}L_2 - 4k_a^{(i)}k_b^{(i)}L_2 - 2k_a^{(i)}k_b^{(ii)}L_2}\right] \quad (8)$$

where

$$k_a^{(i)} = \frac{(EI)_{\text{bimorph}}}{L_{\text{bimorph}}^3}, \qquad k_a^{(ii)} = \frac{E_{\text{segment}}I_{\text{segment}}}{L_{\text{segment}}^3},$$

$$k_b^{(i)} = \frac{(EI)_{\text{bimorph}}}{L_{\text{bimorph}}^2}, \qquad k_b^{(ii)} = \frac{E_{\text{segment}}I_{\text{segment}}}{L_{\text{segment}}^2}$$

Therefore, for a given ΔT (obtained using finite element modeling or measurement), Eq. (8) results in the deflection of the end of the flexure. However, this result is not the deflection of the mirror plate itself but as a first approximation, it is within 85% of the plate deflection as shown in Fig. 5, which is the comparison of the deflections obtained using the analytical model of Eq. (8) to pure bimorph model in the voltage range of 4–10 V (voltage range used to operate our micromirrors).

3.2. Finite element modeling

Since the deflection obtained from analytical model is at the flexure tip (not at the center of mirror plate). This is sufficient for a first-order approximation but not if more detailed analysis is required. Furthermore, it is necessary to investigate the mirror plate deformations associated with the thermally induced bending. A finite element model was constructed to perform a more detailed analysis of the micromirror static deflection.

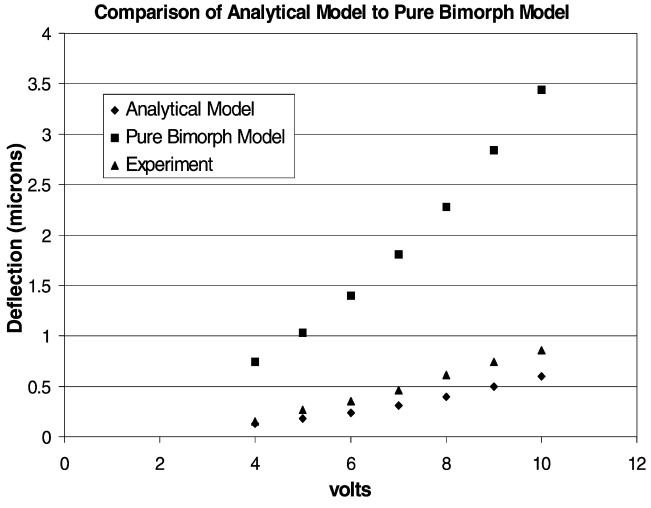

Fig. 5. Deflections predicted by the analytical model compared to those predicted using pure bimorph equations, and experimental data in voltage range of 4–10 V.

A simulation of the micromirror was conducted with a commercially available finite element analysis tool (MARC). The model consists of stacked layers of solid elements with thicknesses that correspond to the actual structural layers fabricated. The simulation consists of an electro-thermal analysis to obtain the temperature distribution resulting from an input electric power. This is then coupled to a mechanical analysis in which the temperature distribution is used to determine deflections resulting from thermal expansion mismatch in a multi-morph structure.

3.2.1. Electro-thermal analysis

An input voltage was applied to the polysilicon heating resistors of micromirror model, which correspond to the two thermal actuators. The other two of the four flexures contain piezoresistors for measuring mirror deflection. Heat transfer paths considered were the thermal conduction to the substrate and to the surrounding air. Both the air and substrate were assumed to remain at room temperature. Convection and radiation through air were not considered, because it has a negligible effect [10]. Only the steady state condition was considered in the analysis, corresponding to a static deflection of micromirror. Fig. 6 shows the vertical temperature profile through the stacked layers of the thermal actuator at various positions along the length of the actuator. The maximum temperature is in the metal layer, thus it contributes the most to actuation. The temperature in the polysilicon and oxide layers decrease along the length of the actuator. Near the base of the actuator, the temperature of the metal and the polysilicon is close, but the difference increases along the length of the flexure.

3.2.2. Thermal–mechanical analysis

The temperature distribution resulting from the electro-thermal analysis was used as an input condition for the thermal–mechanical analysis. Fig. 7 shows the finite element structural model of the micromirror when it is deflecting. Boundary condition is used to fix the location of the beam's base. Fig. 8 shows the results from the analytical model, finite element models and experimental results of mirror deflection versus applied voltage.

4. Micromirror characterization

4.1. Static characterization

4.1.1. Micromirror deflection

Measurements were taken to determine the maximum possible deflection of the micromirror, and the deflection of micromirror versus applied power. Deflection of micromirror was measured over a range of input power by white light interferometric microscope. Measurements were taken

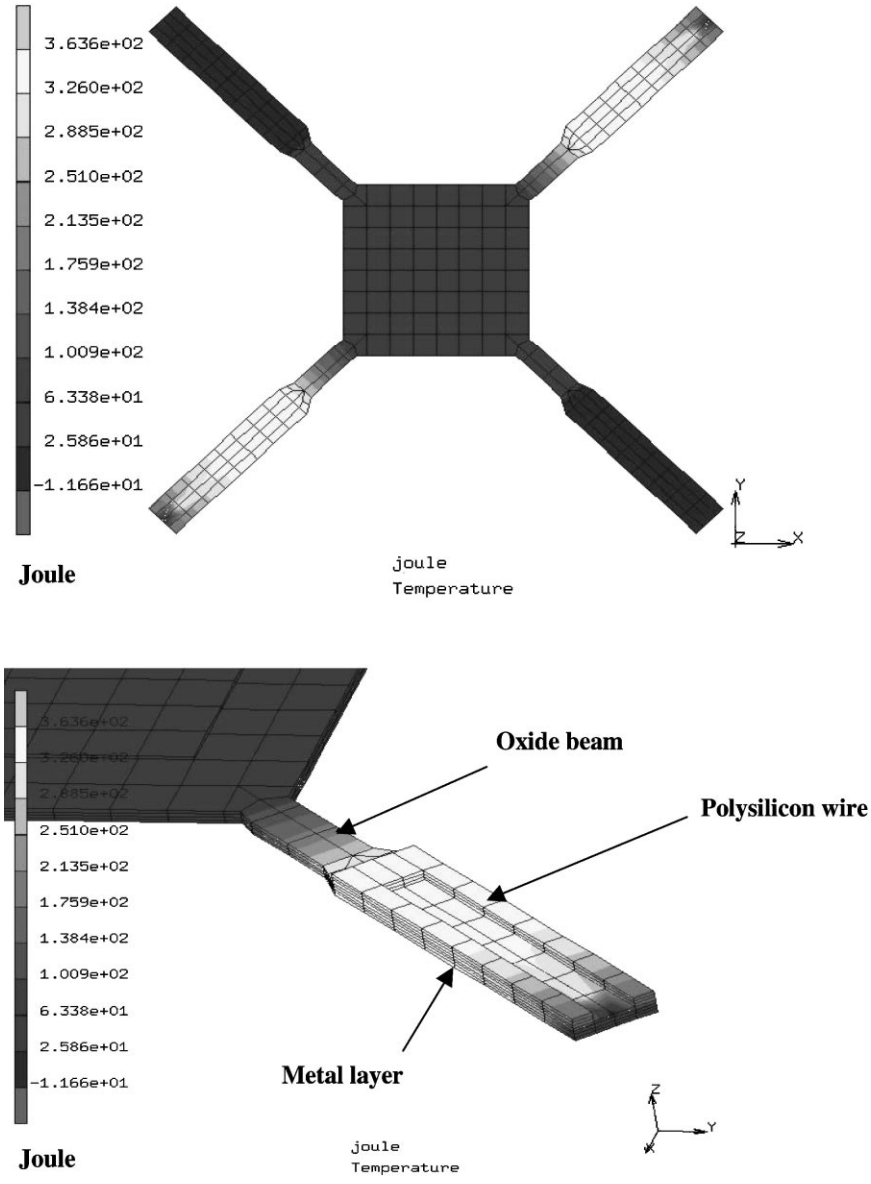

Fig. 6. FEM results showing the vertical temperature profile through the stacked layers comprising the thermal actuator for an applied voltage of 7 V.

on the center of micromirror. Fig. 9 shows the experimentally determined mirror deflection versus applied power. The mirror deflection depends linearly on the drive power with maximum power of 150 mW per pixel at 2 μm deflection with nonlinear effect near zero due to the buckling of heated beam. There is no tilting of the actuated micromirror observed from both simulation and experimental results.

4.1.2. Piezoresistive detection

Deflection of the micromirror is detected with two piezoresistors embedded in the opposing beams. The position of the piezoresistors is at the clamped edges of the beams, where the mechanical stress is highest. The measured change in resistance in a single piezoresistor related to the mirror deflection as a linear relation is shown in Fig. 10. Through Fig. 10, a known relationship may be established to provide the feedback signal for real-time control of micromirror.

4.2. Dynamic characterization

Dynamic measurements were taken to determine the maximum operating frequency of the micromirror. Laser interferometer was setup and used to determine the time required to heat and cool the multi-morph beams. The micromirror was driven by a 4 Hz, 5 V peak input signal. Fig. 11 shows the driving input signal and output signal from photodetector. The upper trace indicates the square wave input and the lower trace indicates the interference fringe movement. The onset of heating or cooling of the beam occurs immediately after applied voltage changes. After the multi-morph beam reaches a steady state temperature, the

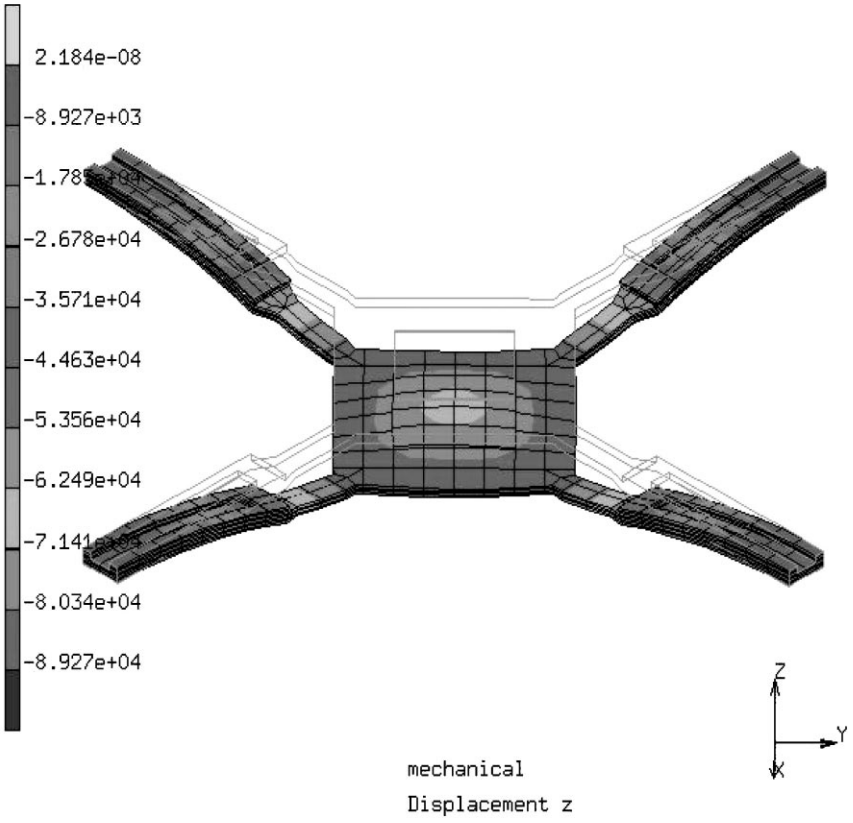

Fig. 7. FEM result showing the deflection distribution of micromirror.

micromirror stops moving and interference pattern stops changing. The heat and cool times for the multi-morph beam are 3 ms, but the encountered force of the oxide beam spring (element 2 in Fig. 4) during micromirror actuation results in an increase of mirror actuation time (heating time = 7 –10 ms). The maximum operating frequency of 100 Hz is achieved. Below this frequency, the multi-morph will completely heat and cool following the drive signal. Above this

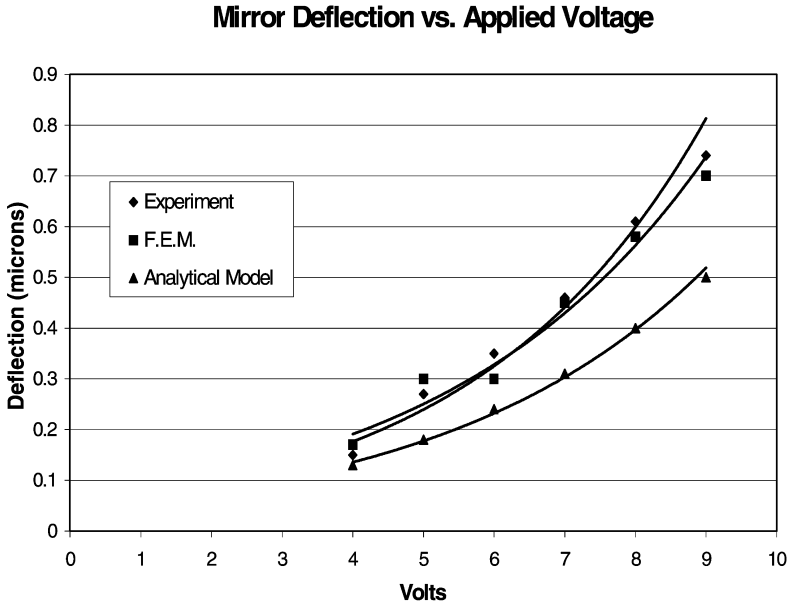

Fig. 8. Mirror deflections obtained from the analytical model, the finite element model, and experimental results in voltage range of 4–10 V.

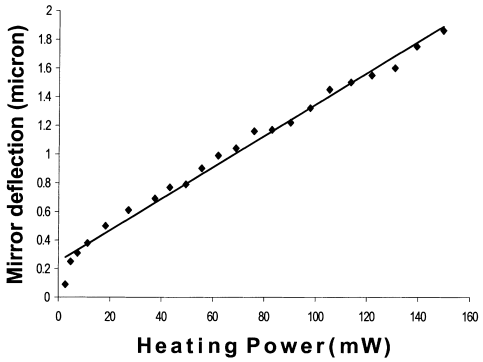

Fig. 9. Micromirror deflection vs. heating power.

maximum frequency, multi-morph beam will not have adequate time to heat and cool and so will not completely deflect in either direction.

5. Micromirror/microlens integration

Using the refractive lenslet array to focus the incident light beam onto only the reflective surface of the mirror is one way to greatly improve the effective optical fill factor with corresponding decrease in static background interference effect. The micromirror in this experiment was designed specifically for use with an available commercial refractive lenslet array from Nippon Sheet Glass Company [15]. In our work, the two-dimensional planar micro lens (PML) is hybrid-integrated directly on top of the micromirror array. Each microlens has a circular shape 250 μm in diameter. The 250 μm center-to-center spacing of the lens array matches with the center-to-center spacing of the micromirror array. The back focal length of the microlens is 560 μm. This lenslet array can provide approximately 90% light transmission at visible wavelengths.

Hybrid flip–chip assembly is applied to integrate the lenslet array on top of the micromirror array. Two glass spacers of 1.925 mm thickness and 1 mm × 14 mm were

Fig. 10. Mirror deflection vs. relative change in resistance of a single piezoresistor.

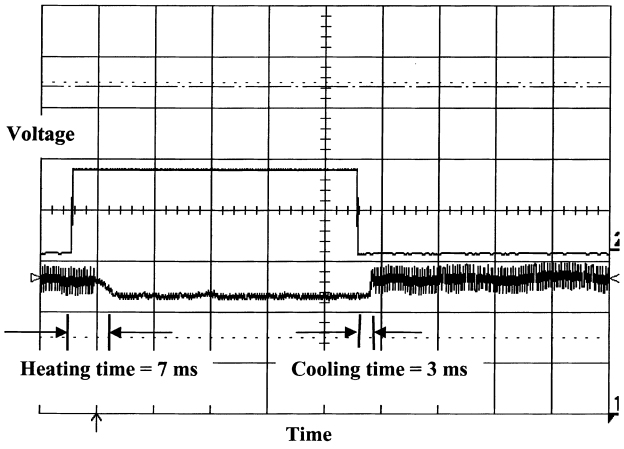

Fig. 11. Experimental result showing input square wave and output interferometer data.

attached to the 16.5 mm × 14 mm quartz window with 20 μm thick UV curable epoxy. The lenslet array was flipped and attached to the quartz window by UV curable epoxy. The quartz window with lenslet array was flip–chip attached to the micromirror package and pre-cured under UV light. The alignment was then adjusted manually in the X and Y position. Afterward, the lenslet array integrated micromirror was investigated under interferometric microscope. Fringe patterns observed by the interferometric microscope were used to correct possible tilt alignment of the lenslet array. The focal point of lenslet was aligned on the center of the micromirror, afterward the epoxy was cured firmly. From observation, the gap between the microlens and micromirror was controlled by the spacers accurately and equals to the focal length of the microlens (error <2% in X–Y–Z position). Fig. 12 shows the close-up of the flip–chip integrated lenslet array on top of the 4 × 4 micromirror array. The final device was packaged in a 40 pin dual-in-line (DIP) package.

6. Phased array beam steering

The optical experimental setup shown in Fig. 13 was used to measure the far-field diffraction pattern of the lenslet integrated micromirror tested for beam steering or aberration correction. The collimated He–Ne laser was used as a signal light source. The beam is folded by mirror M_1 into the optical characterization branch. The beam enters a beam splitter (BS1) and is redirected toward the lenslet integrated micromirror by passing through a pair of lenses L_l and L_s between BS1 and the lenslet integrated micromirror. An iris is located in front of BS1, a focal length away from lens L_l to control beam diameter. The light from the lenslet integrated micro-mirror is reflected back through the afocal telescope (L_l and L_s), BS1 and translating lenses L_{t1} and L_{t2}. The beam enters a Fourier transforming lens L_F and generates the far-field diffraction (point spread function, PSF) on a

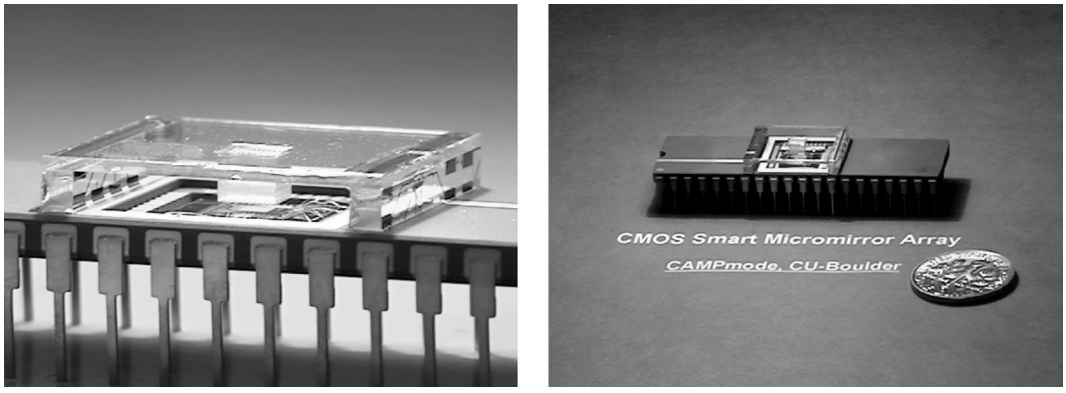

Fig. 12. The lenslet array flip–chip integrated on top of the micromirror array using glass spacers for gap control and the final device packaged in a 40 pins DIP package.

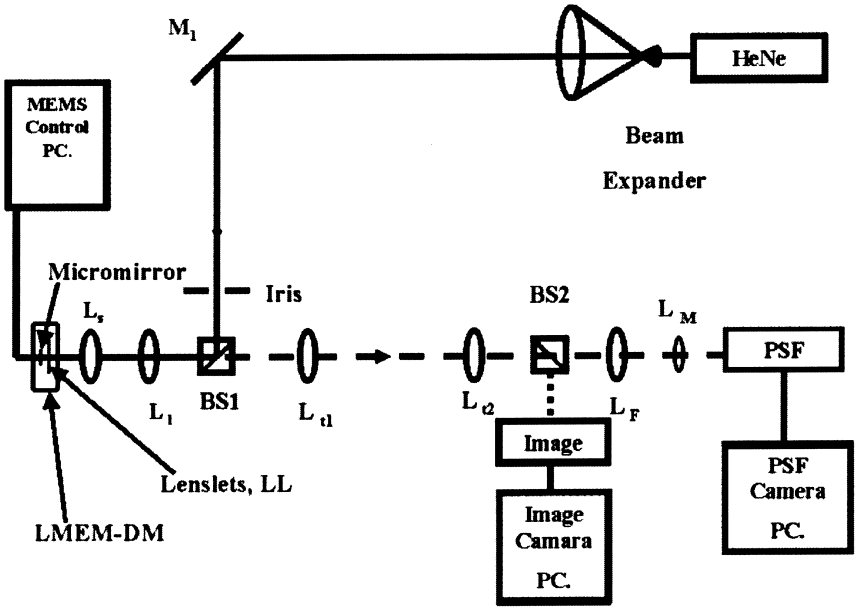

Fig. 13. The optical experimental setup used to measure the far-field diffraction pattern.

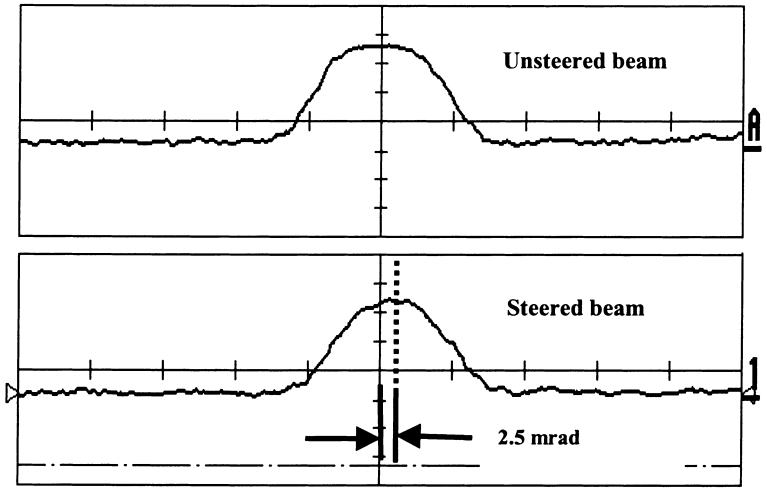

Fig. 14. The beam profiles of unsteered (trace A) and steered beam (trace 1).

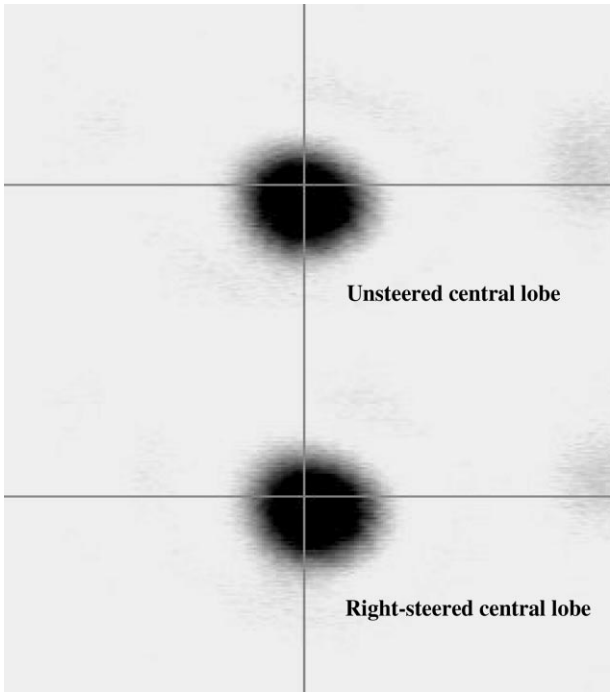

Fig. 15. Central maximum beam steering for a 16 element micromirror array.

256 pixel × 256 pixel CCD camera. Focal lengths of lenses and specification of optical component locations in the experimental setup are listed in [1].

In one-dimension an optical phased array of n elements, with uniform phase shift spacing (between elements) from 0 to 2π rad, steers a beam to an angle $\theta_s = \lambda/nL$, where L is the spacing of the elements (in this case the lenslet dimension), and λ is the operating wavelength. Beam steering of 2.5 mrad from boresight (Figs. 14 and 15) is implemented by a stepped linear ramp pattern across the columns of the micromirror. Steering angle measurements show excellent agreement (within 1% error) with one-dimensional beam steering theory.

7. Conclusions

The phase-only micromirror array has been successfully fabricated by a standard CMOS process. The micromirror is actuated by thermal multi-morph actuators and deflection is detected by piezoresistors. The CMOS switching circuit is integrated adjacent to the individual pixel to address the current to pixel and allow the device to operate in digital mode. A lenslet array is flip–chip hybrid integrated on top of the micromirror to increase the optical fill factor of the system. The hybrid mirror/lenslet array can modulate the light in visible to near infrared wavelengths (400 nm–4 μm wavelength). The device is used to demonstrate optical beam steering ability up to 2.5 mrad.

Acknowledgements

This work was sponsored by the Air Force Office of Scientific Research (AFOSR), Grant No. F49620-98-1-0291. Special thanks to M.A. Michalicek for CMOS circuit discussion and V. Thiantamrong for graphic editing.

References

[1] A. Tuantranont, V.M. Bright, W. Zhang, Y.C. Lee, Flip–chip integration of lenslet arrays on segmented deformable micromirrors, SPIE DTM'99 3680 (1999) 668–678.
[2] A. Tuantranont, V.M. Bright, W. Zhang, Y.C. Lee, Packaging of lenslet array on micromirrors, SPIE 3631 (1999) 156–164.
[3] A. Tuantranont, V.M. Bright, W. Zhang, J. Zhang, Y.C. Lee, Self-aligned assembly of microlens arrays with micromirrors, SPIE 3878 (1999) 90–110.
[4] W.D. Cowan, M.K. Lee, B.M. Welsh, V.M. Bright, M.C. Roggemann, Optical phase modulation using a refractive lenslet array and microelectromechanical deformable mirror, Opt. Eng. 37 (12) (1998) 3237–3247.
[5] R. Krishnamoorthy, T. Bifano, MEMS arrays for deformable mirrors, SPIE 2881 (1996) 35–44.
[6] T.G. Bifano, R.K. Mali, J.K. Dorton, J. Perreault, N. Vandelli, M.N. Horenstein, D.A. Castanon, Continuous-membrane surface micromachined silicon deformable mirror, Opt. Eng. 36 (5) (1997) 1354–1360.
[7] G.D.J. Su, J. Duparre, L. Fan, P.K.C. Wang, M.C. Wu, Micromachined tip-tilt micromirror array with large strokes, Proc. MOEMS (1999) 39–43.
[8] J. Marshall, M. Gaitan, M. Zaghloul, D. Novotny, V. Tyree, J.I. Pi, C. Pina, W. Hansford, Realizing suspended structures on chips fabricated by CMOS foundry processes through the MOSIS service, NISTIR (1994) 5402.
[9] J. Soderkvist, Similarities between piezoelectric, thermal and other internal means of exciting vibrations, J. Micromech. Microeng. 3 (1993) 24–31.
[10] W.H. Chu, M. Mehregany, R.L. Mullen, Analysis of tip deflection and force of a bimetallic cantilever microactuator, J. Micromech. Microeng. 3 (1993) 4–7.
[11] B.C. Read, V.M. Bright, J.H. Comtois, Mechanical and optical characterization of thermal microactuators fabricated in a CMOS process, SPIE 2642 (1995) 22–32.
[12] L. Zhang, G. Yang, Design and FEM simulation: all-light-processing infrared image transducer, SPIE 3878 (1999) 293–301.
[13] T.J. Lardner, R.R. Archer, Mechanics of Solids, McGraw-Hill, New York, 1994.
[14] A.C. Ugural, S.K. Fenster, Advanced Strength and Applied Elasticity, Elsevier, New York, 1987.
[15] R.D. Myers, Planar Microlens Array (PML): Preliminary Specifications, NSG America, Inc., 1998.

Biographies

Adisorn Tuantranont received the BS degree in Electrical Engineering from King Mongkut's Institute of Technology Ladkrabang (KMITL), Bangkok, Thailand, in 1995 and the MS degree in Electrical Engineering (Lasers and Optics) from University of Colorado at Boulder in 1998. He is PhD candidate in Electrical Engineering at University of Colorado at Boulder and working in Optoelectronic Computing Systems Center (OCS) and Center for Advanced Manufacturing and Packaging of Microwave, Optical and Digital Electronics (CAMPmode). His current research interests include MEM deformable micromirror for optical beam steering and shaping, microlens array for optical interconnect, and micromirror for laser resonator and high power applications.

Li-Anne Liew received her BS degree in Mechanical Engineering from the University of Colorado at Boulder in 1998. She is currently a Graduate Research Assistant in the Department of Mechanical Engineering at the University of Colorado, Center for Advanced Manufacturing and Packaging of Microwave, Optical and Digital Electronics (CAMPmode). Her research interests are in the design and packaging of MEMS sensors, MEMS for biomedical applications, and the design and fabrication of MEMS for high-temperature environments.

Victor M. Bright is an Associate Professor of Mechanical Engineering and the Director of the MEMS R&D Laboratory, University of Colorado at Boulder. Prior to joining the University, he was an Associate Professor and the Director of Microelectronics Research Laboratory in the Department of Electrical and Computer Engineering, Air Force Institute of Technology, Wright–Patterson Air Force Base, Ohio (June 1992–December 1997). Prof. Bright's research includes MEMS, silicon micromachining, microsensors, microactuators, MEMS self-assembly, MEMS packaging, optoelectronics, and semiconductor device physics. Dr. Bright received the following awards in the area of MEMS: Best Paper of the MCM'98 — International Conference and Exhibition on Multichip Modules and High Density Packaging, 1998; R.F. Bunshah Best Paper Award at the 1996 International Conference on Metallurgical Coatings and Thin Films. Dr. Bright is a member of IEEE, ASME, and SPIE. He serves on the Executive Committee of ASME MEMS Sub-division.

Wenge Zhang received his BSME degree from Dalian University of Technology in Dalian, China, in 1982 and his MS degree in Mechanical Engineering from the University of Colorado, Boulder in 1995. He joined the University in 1991 and is currently a Research Associate for the Center for Advanced Manufacturing and Packaging for Microwave, Optical and Digital Electronics, at the University of Colorado. His research interests include low-cost prototyping and thermal management of MCMs, thermosonic flip–chip bonding and optoelectronics packaging. He has 14 years of research experience in mechanical design, computer control systems and logic circuit design and 5 years of research experience in thermosonic flip–chip bonding, MCM substrate fabrication and optoelectronics packaging.

Y.C. Lee received his BSME degree from the National Taiwan University in 1978, and the MS and PhD degrees from the University of Minnesota, in 1982 and 1984, respectively. Prof. Lee is a Professor of Mechanical Engineering and the Associate Director of the NSF Center for Advanced Manufacturing and Packaging of Microwave, Optical and Digital Electronics, University of Colorado at Boulder. Prior to joining the University in 1989, he was a Member of Technical Staff at AT&T Bell Laboratories, Murray Hill, NJ. Prof. Lee's research activities include low-cost prototyping and thermal management of multichip modules, 3-D packaging, self-aligning soldering, fluxless or solderless flip–chip connections, optoelectronics packaging, microelectromechahical systems (MEMS), and process control using fuzzy-logic models. His teaching activities include design of mechanical components, senior design projects, integrated manufacturing systems, mechatronics, MEMS, robotics, and electronic/optoelectronic packaging.